Physica B: Condensed Matter 571 (2019) 301–306

Contents lists available at ScienceDirect

Physica B: Condensed Matter

journal homepage: www.elsevier.com/locate/physb

A hybrid product-multi-scale model for magneto-elastic behavior of soft magnetic materials

B. Sai Ram[a,*], A.P.S. Baghel[a,b], S.V. Kulkarni[a], K. Chwastek[c], L. Daniel[b]

[a] Department of Electrical Engineering, Indian Institute of Technology Bombay, Mumbai, 400076, India
[b] Group of Electrical Engineering - Paris (GeePs), UMR CNRS 8507, CentraleSupélec, Univ. Paris-Sud, Université Paris-Saclay, Sorbonne Université, 3 & 11 Rue Joliot-Curie, Plateau de Moulon 91192, Gif-sur-Yvette, Cedex, France
[c] Department of Electrical Engineering, Czestochowa University of Technology, Poland

ARTICLE INFO

Keywords:
Magneto-elastic coupling
Product model
Hysteresis
Soft magnetic materials
Multi-scale model

ABSTRACT

Magnetic properties of electrical steels exhibit a strong sensitivity to mechanical stress; this phenomenon is known as magneto-elastic coupling. Mechanical stress affects microstructural features of soft magnetic materials, which in turn leads to a change in their magnetic characteristics. Therefore, the magneto-elastic coupling in these materials needs to be studied and modeled accurately. This paper is devoted to the development of an analytical magneto-elastic hysteresis model. A recently proposed analytical hysteresis model based on Kádár product approach is modified to model the magnetoelastic effects using a multi-scale approach. The proposed model is validated using the quasi-static hysteresis loops measured for a non-oriented (NO) material (M235-35A) subjected to uni-axial compressive stress and tensile stress. The proposed formalism is applicable to model the reversible effects of stress (in elastic range) and it offers a closed form equation. A stress-dependent coercive parameter is introduced in this equation using a simple numerical procedure. Thus the model can be implemented easily in circuit and field analyses.

1. Introduction

Magneto-elastic coupled behavior of electrical steels plays an important role in the performance of electrical machines, particularly when used in high-speed applications [1–5]. The main causes of induced mechanical stress in electrical machines are manufacturing and assembly processes, temperature gradients, or centrifugal forces [2]. The effects of mechanical stress on magnetic behavior can be observed in terms of change in permeability and losses [6]. The relationship between mechanical stress and magnetic properties of soft magnetic materials has been extensively studied [7–12]. The applied stress significantly affects the magnetic domain configuration of magnetic materials [13]. These effects are evident from Fig. 1 in terms of variations in shape of hysteresis loops under various applied stress conditions.

As depicted in the figure, mechanical stress leads to localized bulging of hysteresis loops which is called *kink*, and hysteresis loops at different stress levels pass through points (P_1 and P_2) known as crossing points. The local widening (kink) and the crossing points [12] have attracted attention of different researchers [8–10]. These effects were reported by Bozorth [12], and they were correlated with Villari reversal for iron alloys [12,14,15]. In Ref. [11], the effect of stress on hysteresis loops considering the kink and crossing points is modeled using Brown's stress field and Bozorth stress field. In iron-silicon steel, compressive stress affects the properties more significantly compared to tensile stresses [16]. In the present work, modeling of hysteresis loops under moderate compressive and tensile stresses is investigated.

Numerous modeling approaches are available in literature to approximate magneto-elastic hysteresis loops [17–20]. Most of them are developed through extensions of classical hysteresis models [17] such as Jiles-Atherton [18] and Preisach formalisms [19]. Their applicability is limited to isotropic materials for short range strains/stresses, and multi-axial stresses are rarely considered. Another approach known as multi-scale (MS) approach is based on an energy equilibrium which considers exchange energy, magneto-crystalline energy, magneto-static energy, and elastic energy [20]. Hysteresis effects are included in the MS approach by adding an irreversible magnetization derived from an approach given in Ref. [21]. This strategy can be successfully applied to multi-axial stress configurations. However, it needs special attention in its numerical implementation. A simplification in the MS approach for a unidirectional magnetic field case provided an anhysteretic magnetization function [22] that could be used as a basis for magneto-elastic hysteresis models.

* Corresponding author.
E-mail address: sairam.eng10@gmail.com (B. Sai Ram).

https://doi.org/10.1016/j.physb.2019.06.069
Received 15 January 2019; Received in revised form 25 May 2019; Accepted 30 June 2019
Available online 01 July 2019

This work deals with an extension of a recently proposed analytical hysteresis model [23] in order to consider magneto-elastic effects. The model has been developed using the Kádár product approach with the modulated sum of a linear reversible (βH) term and a non-linear irreversible (tanh also known as $T(x)$ model [24–26]) term, which is called hybrid 'product—$T(x)$' model [23]. The $T(x)$ model can be considered as a close approximate of the Langevin and Brillouin functions [27]. It can also be applied in its inverse form as B is considered as the input and H as the output of the model [27]. Moreover, using hyperbolic distribution in the Everett integral of the classical Preisach model, it can be evaluated analytically [28]. The model needs standard magnetic parameters such as maximum magnetization, coercivity, and initial differential permeability. An analytical function (in terms of hyperbolic functions) for the anhysteretic magnetization is derived using the MS approach [22]. The present model considers magneto-elastic effects using an anhysteretic function derived from the MS approach as an irreversible magnetization component in the Kádár product approach. Effect of stress is also considered in the very low field region using a modified reduced Rayleigh constant. The well-observed crossing points and the kink are modeled through the coercive force parameter using a Gaussian function [29]. A closed form expression is derived as a hybrid 'product-MS' model and kink effects are then considered in the model using a simple numerical procedure in order to predict complex magneto-elastic behavior. The model parameters are identified using measured hysteresis loops at two stress levels (for compressive stress: 0 and 30 MPa and for tensile stress: 0 and 30 MPa). The computed hysteresis loops at other stress levels are in close agreement with the measured loops.

2. Effect of mechanical stress on magnetization process

Numerous studies on the effect of mechanical stress on microstructural features of soft magnetic materials have been reported in literature [13, 30–33]. Due to the complicated variations in microstructural features of a material under stress, the coupled magneto-elastic behavior cannot be explained fully with change in domain configurations [30]. The main mechanism of the process of magnetization has three steps [31]: (i) Domain wall motion due to stress induced pressure on 90^0 domain walls, (ii) variation in energy of some pinning sites, (iii) change in domain structure in an irreversible manner and (iv) rotation of the magnetization out of the easy axes due to magneto-elastic energy contribution. Diversified nature of pinning sites makes it difficult to consider the effects of stress on the energy of pinning sites. The energy of some of the pinning sites that are present in a demagnetized state may increase [33]. In this work, the kink is modeled in terms of a coercive field coefficient using a simple Gaussian function.

3. Magneto-elastic modeling using a hybrid approach

The idea of Kádár product approach is to model the magnetic susceptibility as a modulated sum of reversible and irreversible terms [24]. The analytical anhysteretic magnetization based on MS model [22] is used in the paper as a component of a description similar in spirit to the Kádár product model yielding a simple scalar magneto-elastic model. The MS and Kádár product models are briefly discussed in the following subsections.

3.1. Analytical anhysteretic magnetization based on multi-scale approach

An analytical anhysteretic magnetization is derived in Ref. [22] for isotropic magnetic materials considering magneto-mechanical coupling for multi-axial stresses. The expression for anhysteretic magnetization derived from the volume fraction of domains (based on the Boltzmann probability function) along an ith (i is x, y, and z) direction is [22]:

$$M_{an} = M_s \frac{A_x \sinh(\kappa H)}{A_x \cosh(\kappa H) + A_y + A_z} \tag{1}$$

Here, M_s is the saturation magnetization, $\kappa = \mu_0 A_s M_s$, $A_i = e^{\alpha_s \sigma_{ii}}$, $i = x, y, z$; $\alpha_s = 1.5 A_s \lambda_s$ and A_s $(=1/(\mu_0 a M_s)$ where, $a = M_s/3\chi_o)$ is a material parameter associated to the initial susceptibility. On contrary to the original work [22], the present model uses the parameter a instead of χ_0. λ_s is the saturation magnetostriction coefficient

Eq. (1) describes fully multiaxial configurations. It can further be simplified for uniaxial stress conditions. If stress is uniaxial and applied only in the field direction (here x-direction and $A_x = A$, $A_y = 1$, and $A_z = 1$) [22]:

$$M_{an} = M_s \frac{A \sinh(\kappa H)}{A \cosh(\kappa H) + 2}, \; A = e^{\alpha_s \sigma} \tag{2}$$

Therefore, the analytical function (2) is able to compute the anhysteretic magnetization taking into account magneto-elastic couplings in soft magnetic materials for uniaxial stress conditions.

3.2. Kádár product model

The classical Preisach model computes the irreversible component of the magnetization process as it uses the concept of hysteron with rectangular hysteretic characteristics [34]. However, the reversible component is dominant in the magnetization process at low induction levels (M and H both approach zero) and at the reversal points of the loop [36]. If the reversible component is not considered in the model, it may lead to zero susceptibility in the low induction regions. Such kind of problems can be avoided by using the product Preisach model which has been developed by Kádár [35–38]. It is given as [35]:

$$\frac{dM}{dH} = R(M)\left[\beta + \int_{H_o}^{h} Q(h,\ h')dh'\right] \tag{3}$$

Here, β is a reduced Rayleigh constant which represents the initial relative susceptibility and characterizes the reversible domain wall motion [39] resulting in linear changes of the magnetization M with the applied field H. $R(M)$ is a modulating function which modulates shape of minor loops depending upon their relative average magnetization [23]. Following the works of Gans and Kádár, a parabolic function is used for the modulating function. This assumption is equivalent to the consideration of non-linear modulation applied to total susceptibility. By analogy to Eq. (3), an analytical hysteresis model has been proposed recently by the authors in Ref. [23] as:

$$\frac{dy}{dx} = R(y)[\beta + \frac{df}{dx}] \tag{4}$$

Here, y, f, and x represent normalized magnetization, irreversible magnetization, and magnetic field respectively. In Ref. [23], the hyperbolic tangent function was used as the function f in (4). The model (4) can be reduced to Takács model [24] by choosing $\beta = 0$, and $R(y) = 1$. Therefore, it is referred to as the hybrid 'product—$T(x)$' model. The model (4) can also be represented in its inverse form [23]. This hybrid product model is modified using the multi-scale approach to consider coupled magneto-elastic behavior of soft magnetic materials in the following subsection.

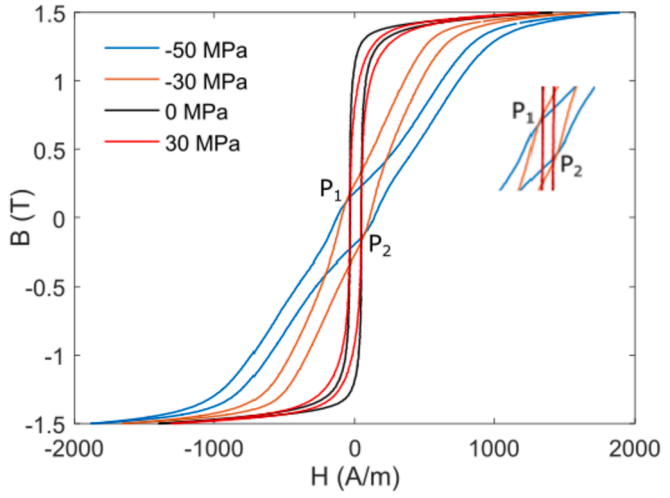

Fig. 1. Effect of compressive stress (negative values) and tensile stress (positive values) on measured hysteresis loops of NO material (M235-35) at 1.5 T and 50 Hz.

3.3. Magneto-elastic hysteresis model

The relationship derived for the anhysteretic magnetization function (2) is here further modified and used as one of the terms in the product model (4) by introduction of a coercive parameter in a manner analogous to the concept reported in Refs. [24,25]. The irreversible magnetization in the normalized form for the uni-axial stress case can be given as:

$$f = \frac{M}{M_s} = \frac{A\,\sinh(\kappa_n h \pm a_0)}{A\,\cosh(\kappa_n h \pm a_0) + 2} \tag{5}$$

Here, f and h represent normalized irreversible magnetization component and magnetic field, respectively. a_o and κ_n are the normalized values of the coercive parameter and κ, respectively. Normalization of magnetic field, κ and a_o is done with $H_{\max}$ (maximum magnetic field or peak values of H waveform). In the above equation + is chosen for the ascending branch and – is chosen for the descending branch. The effect of stress in the Rayleigh region has also been reported in the literature [40,41]. The parameters for Rayleigh law of magnetization may be affected by the applied stress [42]. Although a more complex function for stress-dependent Rayleigh constant could be used to improve accuracy, it increases the number of unknown model parameters. Therefore, we propose to describe the effect of stress on the value of the Rayleigh constant using a linear relationship:

$$\beta_\sigma = \beta_0 + \beta_1\sigma \tag{6}$$

Now, the product model can be rewritten as [37,38]:

$$\frac{dm}{dh} = R(m)[\beta_\sigma + \frac{df}{dh}]$$
$$\int_0^m \frac{dm}{1-m^2} = \int_0^h \beta_\sigma dh + \int_0^h df \tag{7}$$

Here, m is the normalized magnetization. Integrating Eq. (7) with the initial (h_{in}, m_{in}) and current values (h_{cur}, m_{cur}) of m and h variables, it becomes:

$$\tanh^{-1}(m)\big|_{m_{in}}^{m_{cur}} = \beta_\sigma h\big|_{h_{in}}^{h_{cur}} + f\big|_{h_{in}}^{h_{cur}} \tag{8}$$

Here, (h_{cur}, m_{cur}) and (h_{in}, m_{in}) are the normalized current and initial values H and M. $\tanh^{-1}$ is the inverse hyperbolic tangent function which in some computation tools (like Matlab) is represented as atanh. By substituting f from Eq. (5) into (8), it yields

$$\tanh^{-1}(m_{cur}) - \tanh^{-1}(m_{in}) = \beta_\sigma(h_{cur} - h_{in}) + \frac{A\,\sinh(\kappa_n h_{cur} \pm a_o)}{A\,\cosh(\kappa_n h_{cur} \pm a_o) + 2} - \frac{A\,\sinh(\kappa_n h_{in} \pm a_o)}{A\,\cosh(\kappa_n h_{in} \pm a_o) + 2} \tag{9}$$

Now the kink regions are simulated through the 'a_o' parameter using a Gaussian function. Thus the a_o parameter is modified as:

$$a_o = a_{c0}e^{\beta_a\sigma}\left(1 + e^{-((B_{cur-1}+B_{co})/b)^2}\right) \tag{10}$$

Here, a_{c0} is the normalized coercive field at zero stress, $B_{cur\text{-}1}$ is the magnetic field at the previous instant, B_{co} is magnetic flux density at both crossing points, β_a is an exponential parameter that defines variation of the normalized coercive field with stress, and b is a Gaussian function parameter. Since the crossing points and the kink are independent of stress [13], the values of the parameters in (10) are not functions of stress. Thus, the modified model (9) can be referred to as the 'product-MS' model which can consider magneto-elastic coupled behavior of soft magnetic materials. It is worth noting here that the proposed model (9) is a direct model with the input as H field and the output as B field. The value of magnetization (m_{cur}) at every time instant can be determined by (9) using values of h_{cur}, h_{in}, m_{in} and a_o. The values of h_{in} and m_{in} can be chosen as the tip values ($h_{\max}$ and $m_{\max}$) of the major loop [23]. These values will remain constant at all time steps. At the first time step, m and h values are known as $h_{in} = h_{\max} = h_{cur}$ and $m_{in} = m_{\max} = m_{cur}$ and at the second time step, h_{in} (= $h_{\max}$), m_{in} (= $m_{\max}$), and h_{cur} are known and the value of a_o is computed from (10) using $B_{cur\text{-}1}$ which can be determined using m $_{cur\text{-}1}$ and h $_{cur\text{-}1}$ of the previous time step. The true values of magnetization and magnetic flux density in physical units can be calculated from

$$M = M_s m \tag{11a}$$

$$\mathrm{H} = \mathrm{H}_{\max}\mathrm{h} \tag{11b}$$

$$B = \mu_0(H + M) \tag{11c}$$

Moreover, the model can be used in its original and inverse variants (considering H as output and B as input to the model) [23]. The inverse model can be derived using (7) and 11(c) as follow:

$$\frac{dm}{db} = \frac{dm/dh}{\mu_0(1 + dm/dh)} \tag{12}$$

where dm/dh is given by (7). The model in its inverse form (12) can be solved numerically [23]. The model also has the ability to consider multiaxiality (stress tensor in two or three dimensions) as evident in (1). However, Eqs. (6) and (10) would also need to be modified to take into account multiaxial configurations. This could be done using the concept of equivalent stress [43]. In such an approach, a fictitious uniaxial equivalent stress (since it is a scalar value) is defined from the multiaxial stress tensor using an equivalence criterion. This uniaxial stress is assumed to have a similar effect as the actual multiaxial stress. This concept has for instance been successfully applied to describe the effects of stress on the magnetic susceptibility of magnetic materials [44,45], or on the hysteresis losses in iron-silicon steels [46,47]. More complex, fully multiaxial approaches, could be defined but they would indeed require replacement of the scalar value describing the stress by a tensorial expression (for instance using the magneto-elastic energy as a variable instead of the stress).

4. Results and discussion

Measurements of hysteresis loops are carried out on Fe-Si non-oriented material (grade: M235-35A) samples at induction levels (1.0 T and 1.5 T) with pure sinusoidal flux density at 50 Hz using a single sheet tester (SST) [20]. Mechanical stresses are applied using pneumatic tension and compression units of the SST. Modeling is done for quasi-

Table 1
Model parameters for compressive stress and tensile stress.

Parameter	*Compressive*	*Tensile*
M_s (A/m)	1.35×10^6	1.35×10^6
κ (m/A)	0.0161	0.0185
a_{co}	0.029	0.029
b (T)	0.01	110
β_a (MPa^{-1})	0.02	3×10^{-4}
B_{co} (T)	0.2	0.2
β_0	0.04	0.04
β_1 (Pa^{-1})	8.2×10^{-11}	1.5×10^{-15}
λ_s	1.5×10^{-6}	1.5×10^{-6}

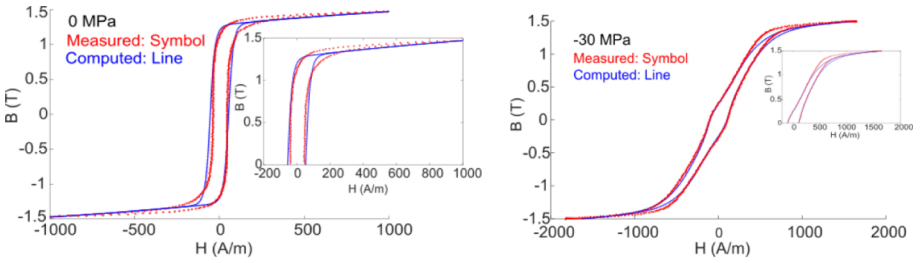

(a) (b)

Fig. 2. Comparison of measured and computed hysteresis loops at 1.5 T under compressive stress of (a) 0 MPa (b) 30 MPa.

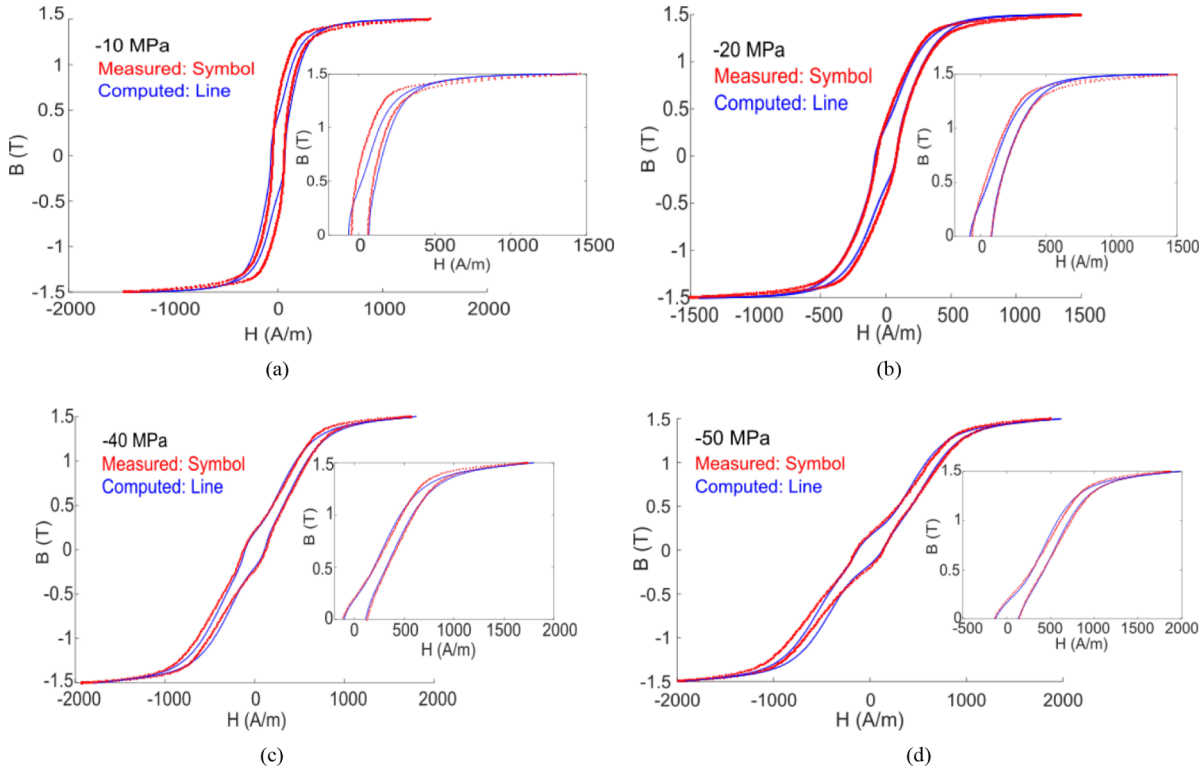

(a) (b) (c) (d)

Fig. 3. Comparison of measured and computed hysteresis loops at 1.5 T under compressive stress of (a) −10 MPa (b) −20 MPa (c) −40 MPa (d) −50 MPa.

static conditions as the frequency-dependence is neglected in this work. The model parameters (10) are determined using the lsqcurvefit function in Matlab®, using measured hysteresis loops at two stress levels (0 and ± 30 MPa). It should be noted that positive and negative values of stress correspond to tensile stress and compressive stress respectively. Silicon Iron materials have a magnetostriction coefficient of the order of a few 10^{-6}. The value of $\lambda_s = 1.5 \times 10^{-6}$ has been identified to fit the results for M235-35A within reasonable accuracy [22]. The optimized parameters are given in Table I.

Comparison of measured and computed hysteresis loops at stress levels (0 and −30 MPa) is shown in Fig. 2.

The model is then applied to predict hysteresis loops at other compressive stress levels using the optimized parameters in Table I. Measured and computed hysteresis loops are shown in Fig. 3.

Similarly, the model parameters for tensile stress (third column of Table I) are determined by using the two stress levels (0 and 30 MPa). These model parameters are used to predict hysteresis loops for a tensile stress of 50 MPa. Comparison of computed and measured hysteresis

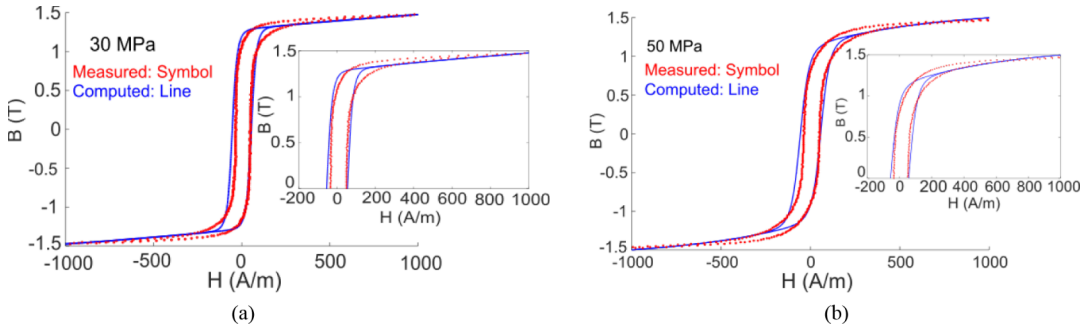

(a) (b)

Fig. 4. Comparison of measured and computed hysteresis loops at 1.5 T under tensile stress of (a) 30 MPa (b) 50 MPa.

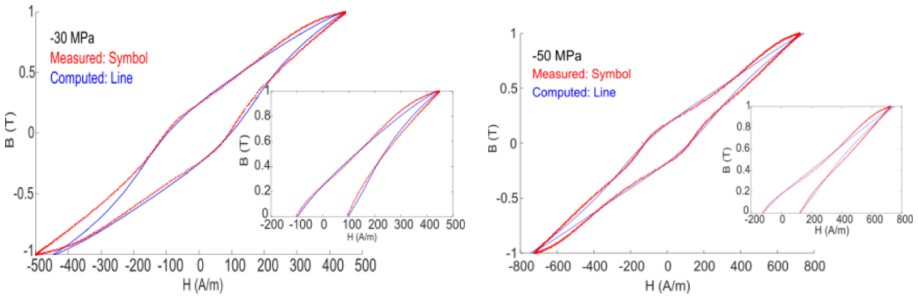

(a) (b)

Fig. 5. Comparison of measured and computed hysteresis loops at 1.0 T under compressive stress of (a) −30 MPa (b) −50 MPa.

Table 2
Normalized root mean square error for different stress levels.

Stress (MPa)	−50	−30	0	30	50
% NRMS error	15.1	16.5	17.6	15.1	14.2

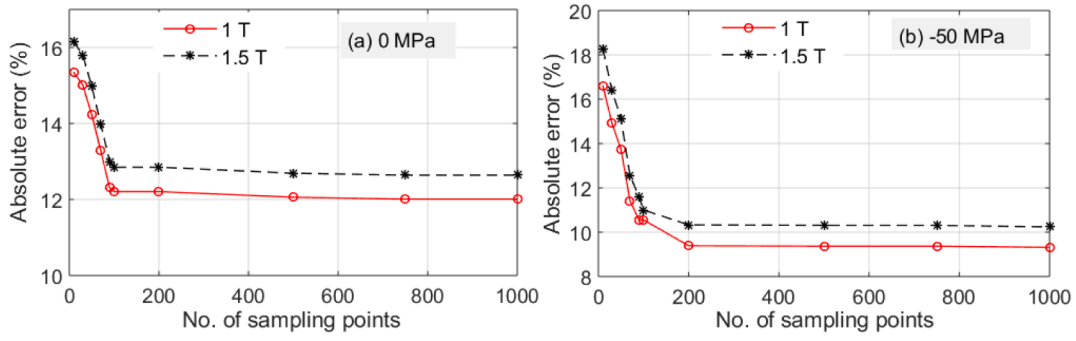

(a) (b)

Fig. 6. Percentage error in computed losses with number of samples at different induction levels (a) 0 MPa (b) −50 MPa.

loops is given in Fig. 4.

The proposed method has also been applied to predict the hysteresis loops at lower induction levels (minor loops). A comparison of computed hysteresis loops at 1.0 T for two compressive stress levels with measured is shown in Fig. 5.

Normalized Root Mean Square (NRMS) % errors for loops at different stress levels are computed using the following equation as:

$$NRMS\ Error = \frac{1}{M_s}\sqrt{(\sum_{i=1}^{n}(M_{exp} - M_{comp})^2)/n} \quad \times \quad 100 \tag{13}$$

Here, M_{exp} and M_{comp} are the measured and computed magnetizations, and n is the number of data points on the loop. The maximum % NRMS error normalized with M_s is not higher than 18% for the considered stress levels. % NRMS Errors for different stress levels are given in Table II.

It is interesting to note that the maximum error is at the zero stress level even though the measured data of the same stress is used for parameter identification. Moreover, it can also be observed from Table II that the error decreases as the stress increases. This might be attributed to the highly steep and gooseneck shape of the loops of lower stress levels. Therefore, inaccuracies may occur due to fitting complex

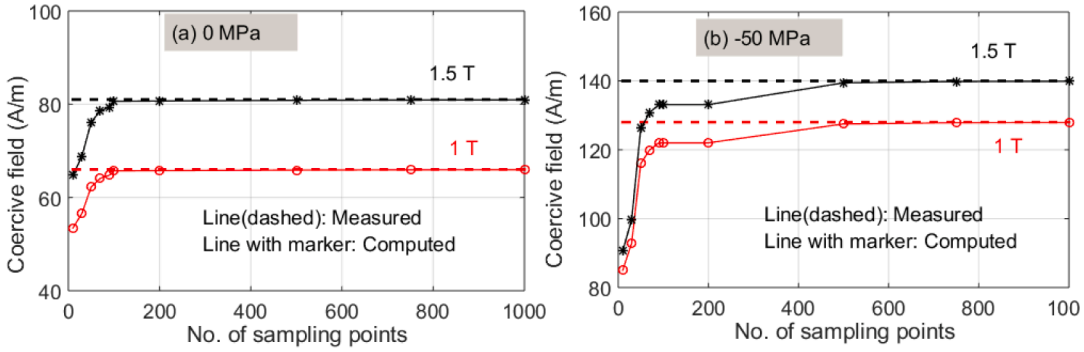

(a) (b)

Fig. 7. Variation of computed coercive field with number of samples at different induction levels (a) 0 MPa (b) −50 MPa.

shapes with a rather simplified analytical model. Moreover, an analysis to assess the effect of sampling on the accuracy of computed results is also performed to model hysteresis loops with different B_{max} values at different stress levels as shown in Fig. 6 (a)-(b). It can be observed from the figure that the accuracy of the computed losses increases as the number of samples increases. The improvement occurs up to a certain number of samples (200 here) after which no significant improvement is observed. Despite accurate loss computation, the simulated hysteresis loop may not be fitted correctly due to kinks in lower induction regions. The variations in the computed coercive field values with respect to measured ones are shown in Fig. 7 (a)-(b). It is clearly visible from these figures that the accurate evaluation of the coercive field and the loop shape needs a higher number of sampling points at higher stress levels. Therefore, it is advisable to choose at least 200 samples per cycle for a precise hysteresis modeling for unstressed conditions and at least 500 points at higher stress levels.

5. Conclusion

This paper is devoted to the development of a simple analytical magneto-elastic hysteresis model using the multi-scale and Kádár product approaches. An analytical function for anhysteretic magnetization derived from a multi-scale approach is modified in order to consider irreversible hysteresis effects. The function is then used as the irreversible term in the proposed product model. The influence of compressive stress on pinning densities is modeled via the coercive field parameter using a Gaussian function. Stress effects in the Rayleigh region of low field values are also considered. The model can predict hysteresis loops in reasonably close agreement with measured hysteresis loops for stress levels (both compressive and tensile stress). It provides a relatively simple differential form (9) for the description of complex magneto-elastic material behavior and also offers easy numerical implementation in circuit and field analyses. Effect of sampling on the computed loss is also discussed in the paper. A further improvement in the model is possible with a detailed study of its reversible component behavior under applied mechanical stress. Extensions of the proposed model for taking into account multi-axial stress conditions and frequency-dependence behavior is considered as a part of future research.

Acknowledgements

The authors would like to thank the COCTEL project Piloted by RENAULT-SAS, Guyancourt, France and financed by the ADEME. They would like to thank Indian National Academy of Engineering (INAE), India for support under INAE Chair Professorship Scheme and IIT Bombay, Mumbai, India for IRCC Research Award Grant.

References

[1] A. Belahcen, IEEE Trans. Magn. 41 (2005) 1624.
[2] L. Bernard, L. Daniel, IEEE Trans. Magn. 51 (2015) 7002513.
[3] S. Zeze, Y. Kai, T. Todaka, M. Enokizono, IEEE Trans. Magn. 48 (2012) 3352.
[4] X. Liu, G. Slemon, IEEE Trans. Energy Convers. 6 (1991) 492.
[5] Y. Xiao, P. Zhou, M. Rosu, Proc. IEEE Int. Electr. Mach. Drives Conf. (May 2017), pp. 1–6 Miami, FL, USA.
[6] A.J. Moses, J. Mater. Sci. 9 (1974) 217.
[7] B.D. Cullity, C.D. Graham, Introduction to Magnetic Materials, IEEE Press, John Wiley & Sons, Inc., Canada, 2009.
[8] C.S. Schneider, J. Appl. Phys. 97 (2005) 10E503.
[9] M. Le Floc'h, A. Globus, J. Appl. Phys. 61 (1987) 4850.
[10] O. Perevertov, R. Schaefer, J. Phys. D 47 (2012) 185001.
[11] O. Perevertov, J. Magn. Magn. Mater. 428 (2017) 223.
[12] R.M. Bozorth, Ferromagnetism, Van Nostrand, New York, 1951.
[13] D.P. Bulte, A. Langman, J. Magn. Magn. Mater. 251 (2002) 229.
[14] E. Villari, Annu. Rev. Phys. Chem. 126 (1865) 87.
[15] R.M. Bozorth, H.J. Williams, Rev. Mod. Phys. 17 (1945) 72.
[16] A.P.S. Baghel, J.B. Blumenfeld, L. Santandrea, G. Krebs, L. Daniel, J. Electr. Eng. (2019) Under review.
[17] T. Suzuki, E. Matsumoto, J. Mater. Process. Technol. 161 (2005) 141.
[18] M.J. Sablik, D.C. Jiles, IEEE Trans. Magn. 29 (1993) 2113.
[19] C. Appino, G. Durin, V. Basso, C. Beatrice, M. Pasquale, G. Bertotti, J. Appl. Phys. 85 (1999) 4412.
[20] L. Daniel, M. Rekik, O. Hubert, Arch. Appl. Mech. 84 (2014) 1307.
[21] H. Hauser, J. Appl. Phys. 96 (2004) 2753.
[22] L. Daniel, IEEE Trans. Magn. 49 (2013) 2037.
[23] K. Chwastek, A.P.S. Baghel, B. Sai Ram, B. Borowik, L. Daniel, S.V. Kulkarni, J. Phys. D 51 (2018) 145003.
[24] J. Takács, COMPEL 20 (2001) 1002.
[25] J. Takács, COMPEL 37 (2018) 1131.
[26] J. Takács, Mathematics of Hysteretic Phenomena, Wiley-VCH, Berlin Germany, 2003.
[27] J. Takács, COMPEL 36 (2017) 850.
[28] J. Takács, The everett integral and its analytical approximation, in: L. Malkinski (Ed.), Advanced Magnetic Materials, INTECH, Rijeka, 2012, p. 203 Ch. 8.
[29] B. Sai Ram, A.P.S. Baghel, S.V. Kulkarni, L. Daniel, Accepted for Presentation in COMPUMAG, (2019).
[30] D.J. Craik, M.J. Wood, J. Phys. D 4 (1971) 1009.
[31] D.C. Jiles, J. Phys. D 28 (1995) 1537.
[32] R. Birss, IEEE Trans. Magn. 7 (1971) 113.
[33] D.C. Jiles, D.L. Atherton, J. Phys. D 17 (1984) 1265.
[34] I.D. Mayergoyz, Mathematical Models of Hysteresis, Springer Science & Business Media, 2012.
[35] G. Kádár, Phys. Scripta T25 (1989) 161.
[36] E. Della Torre, J. Oti, G. Kádár, IEEE Trans. Magn. 26 (1990) 3052.
[37] G. Kádár, Physica B 275 (2000) 40.
[38] E. Della, Torre, Magnetic Hysteresis, IEEE Press, Piscataway, 1999.
[39] G. Bertotti, Hysteresis in Magnetism for Physicists, Material Scientists and Engineers, Academic Press, San Diego, 1998.
[40] R.R. Birss, IEEE Trans. Magn. 7 (1971) 113.
[41] L. Li, D.C. Jiles, J. Appl. Phys. 93 (2003) 8480.
[42] M. Kachniarza, A. Bieńkowskib, J. Salachb, R. Szewczykb, Acta Phys. Pol. 133 (2018) 1056.
[43] L. Daniel, O. Hubert, IEEE Trans. Magn. 46 (2010) 3089.
[44] G. Krebs, L. Daniel, IEEE Trans. Magn. 48 (2012) 2488.
[45] P. Rasilo, U. Aydin, F. Martin, A. Belahcen, R. Kouhia, L. Daniel, IEEE Trans. Magn. 55 (2019) 2002104.
[46] M. Rekik, L. Daniel, O. Hubert, IEEE Trans. Magn. 50 (2014) 2001604.
[47] K. Yamazaki, H. Mukaiyama, L. Daniel, IEEE Trans. Magn. 54 (2018) 1300304.